

Order-disorder mechanism of the I-II phase transition in CsZnPO₄

Isao Yamashita,¹ Hitoshi Kawaji,¹ Tooru Atake,¹ Yoshihiro Kuroiwa,^{1,2}
and Akikatsu Sawada^{1,2}

¹*Materials and Structures Laboratory, Tokyo Institute of Technology, 4259 Nagatsuta-cho, Midori-ku, Yokohama, 226-8503 Japan*

²*Department of Physics, Faculty of Science, Okayama University, 3-1-1, Tsushima-naka, Okayama, 700-8530 Japan*

(Received 11 June 2002; published 16 January 2003)

The I-II phase transition in CsZnPO₄ was studied by x-ray powder diffractometry with high-energy synchrotron radiation and by differential scanning calorimetry (DSC). The Rietveld analysis of the diffraction data and the electron density studies by the maximum entropy method showed substantial disorder at oxygen sites in the highest-temperature phase I. From the DSC experiments, the enthalpy of the I-II phase transition was estimated as 715 J mol⁻¹ and the entropy of transition as 1.2 J mol⁻¹ K⁻¹, which should be comparable with $R \ln 2 = 5.76 \text{ J K}^{-1} \text{ mol}^{-1}$. These results imply an order-disorder mechanism for the I-II phase transition in CsZnPO₄. Phase II is considered as so-called weak ferroelectrics, and the primary order parameter might be given by the orientation ordering of ZnO₄ and PO₄ tetrahedra.

DOI: 10.1103/PhysRevB.67.014104

PACS number(s): 64.70.Kb, 65.40.Ba

I. INTRODUCTION

CsZnPO₄ (CZP), a member of the phosphate family having trydimite type structure,¹ has successive phase transitions at 220, 533, and 583 K due to the phase sequence of IV → III(*P2₁/a*) → II(*Pn2₁/a*) → I(*Pnma*).²⁻⁵ Recently we found an abnormally large thermal hysteresis for the lowest-temperature phase transition III-IV.^{4,5} The room-temperature phase III is easily supercooled down to liquid helium temperature and the metastable phase III transforms to the stable phase IV very slowly below the phase transition temperature 220 K; in fact it took more than 100 h at 195 K.⁵ In the course of the studies on the properties of CZP, we found also anomalous structural properties in the highest-temperature phase I, and thus we have extended the detailed studies to higher-temperature phases.

Blum *et al.*³ have reported that the crystal structures of phases I, II, and III are very similar to those of NH₄LiSO₄ (ALS).⁶⁻⁸ The highest-temperature phase I of ALS is in disordered state with respect to oxygen sites,^{8,9} and the I-II phase transition is a type of ferroelectric phase transition. The primary order parameter for the transition is the orientation ordering of SO₄ tetrahedra.¹⁰

On the analogy of structures of CZP and ALS, phase II of CZP should be ferroelectric, and the I-II phase transition is considered as a ferroelectric phase transition. A small hump was observed in the dielectric constant of CZP at the I-II phase transition, but the temperature dependence of the permittivity does not follow the Curie-Weiss law.² Although the highest-temperature phase I of CZP has been reported as to be in an ordered state,³ the atomic displacement parameter of oxygen atoms is abnormally large, which implies a large amplitude of the thermal motion and/or existence of several stable sites for positional displacement in phase I.

The related compounds ALS (Ref. 10) and CsCoPO₄ (Ref. 2), are so-called weak ferroelectrics. Although the origin of the weak ferroelectric phase transition is still under argument, it should be of intermediate nature between order-disorder and displacive type. For example, in the case of typical weak ferroelectrics Li₂GeO₇O₁₅, a dielectric critical

slowing down has been observed,^{11,12} which implies a order-disorder type of mechanism. On the other hand, Raman scattering and far-infrared absorption measurements have shown a soft mode,^{13,14} which should be ascribed to a displacive type of phase transition. Similar behavior was observed in another weak ferroelectrics (CH₃NHCH₂COOH)₃CaCl₂.¹⁵⁻¹⁷ In order to clarify the mechanism of the weak ferroelectric transition, a microscopic study from the viewpoint of the electron density distribution is strongly required. The I-II phase transition in CZP is a candidate for the weak ferroelectric phase transition. In the present study, the detailed structures were determined by powder x-ray diffractometry with high-energy synchrotron radiation. The Rietveld analysis of the diffraction data and electron density studies by the maximum entropy method (MEM) showed substantial disorder at oxygen sites in the highest-temperature phase I. The thermal properties were also studied by differential scanning calorimetry (DSC), and the transition enthalpy and entropy were estimated.

II. EXPERIMENT

The single crystals of CZP were synthesized by a flux method.⁵ The particles larger than 0.2 mm were separated from the product, and they were used for the present experiments. The chemical composition of the sample was determined by inductively coupled plasma (ICP) analysis as Cs_{1.00}Zn_{0.99}PO₄, and no impurity was detected. For the powder x-ray diffraction with synchrotron radiation, a small amount of sample was ground in an agate mortar into fine powder of about 10 μm. The fine powder was put into ethanol. After stirring, the supernatant part was sucked up with a syringe. Thus, by evaporating ethanol, a very fine powder of CZP with uniform particle size was obtained. The fine powder was put into a quartz capillary of 0.3 mm inside diameter, which was used for the x-ray diffraction. The powder diffraction experiments were carried out with a large Debye-Sherrer camera¹⁸ installed at BL02B2 in the synchrotron radiation facility SPring-8, Japan. High-energy x rays

TABLE I. Results of the Rietveld analysis of phase I (disordered model). $Pnma$ $a=9.2335$ (3) Å, $b=5.4603$ (2) Å, $c=9.3518$ (3) Å, and $T=613$ K. The form of the anisotropic temperature factor is exp $[-2\pi^2(h^2a^*U_{11}+k^2b^*U_{22}+l^2c^*U_{33}+2hka^*b^*U_{12}+2hla^*c^*U_{13}+2klb^*c^*U_{23})]$.

Site	g (σ)	Atoms	x (σ)	y (σ)	z (σ)	U (σ) (10^{-2} Å ²)
4c	1.0	Cs	0.0027 (1)	0.25	0.1975 (1)	3.7 ^a
4c	1.0	Zn	0.1718 (2)	0.25	0.5834 (3)	2.2 ^a
4c	1.0	P	-0.1924 (5)	0.25	-0.4102 (9)	3.3 ^a
4c	1.0	O1	-0.029 (1)	0.25	-0.3971 (9)	7.2 ^a
4c	1.0	O2	-0.265 (2)	0.25	-0.275 (2)	12.7 ^a
8d	0.50 (1)	O31	-0.24952 (5)	-0.00340 (2)	-0.45225 (1)	1.5 (1)
8d	0.50	O32	-0.24322 (5)	0.07136 (2)	-0.52755 (1)	= U_{O31}

^aEquivalent isotropic thermal parameter, U_{eq} .

with wavelength $\lambda=0.5$ Å were used as the incident x rays. The wavelength of the incident x rays was confirmed using standard CeO₂ (SRM674a). The diffraction patterns of the sample were recorded on an imaging plate in transmission geometry. The measurements were carried out at 613 K for phase I and at 553 K for phase II. The diffraction data were analyzed by the Rietveld method¹⁹ with the program RIETAN-2000.²⁰ In order to avoid local minima, the calculation was carried out with the conjugate direction method through refinement. The contribution of the background caused by the quartz capillary was subtracted from the primary diffraction data. The split pseudo-Voigt function was used for the profile function. The difference Fourier synthesis and the MEM analysis were carried out using the programs FOUSYN and MEED.²¹

The differential scanning calorimetry (DSC) was carried out using Perkin-Elmer Pyris 1. The powder sample was prepared by grinding a piece of single crystal into a fine size of $d \leq 32$ μm. The amount of powder sample loaded into the aluminum pan was 14.29 mg. The DSC measurements were carried out in the temperature range from 300 K to 673 K with a scanning rate of ± 5 K min⁻¹. To obtain quantitative data from the DSC measurements, the calibration was performed with the melting of indium and zinc.

III. RESULTS AND DISCUSSION

The x-ray diffraction data of phase I were analyzed by the Rietveld method, where the structure parameters with isotropic atomic displacement reported by Blum *et al.*³ were used for the initial structure. The data up to $2\theta=40^\circ$, which corresponds to 0.73 Å in d spacing, were used for the analysis. The refined structure is in good agreement with that of Blum

*et al.*³ The reliability factors—the weighted profile, Bragg intensity, and goodness-of-fit indicator¹⁵—are $R_{wp}=3.15\%$, $R_1=3.00\%$, and $S=1.43$, respectively. The abnormally large thermal displacement parameters are observed for oxygen atoms, which were also reported by Blum *et al.*³

The residual electron density around O(3) atoms in the difference Fourier synthesis map of phase I showed clearly double peaks, which implied positional disorder. Thus further refinement was made by using the split-atom method for O(3) atoms; the O(3) atoms are split into 8d sites O(31) and O(32), where the occupancy probabilities (g) of O(31) and O(32) should be 1 in total as $g_{O(31)}+g_{O(32)}=1$.

Table I shows the results of the revised Rietveld analysis of phase I, where the anisotropic thermal displacement parameters were applied for Cs, Zn, P, O(1), and O(2) atoms, and the isotropic atomic displacement parameters with $U_{O(31)}=U_{O(32)}$ were applied for O(31) and O(32). The refined anisotropic thermal parameters are listed in Table II. Figure 1(a) illustrates the profile fit and the difference patterns of the revised Rietveld analysis of phase I. The reliability factors are $R_{wp}=2.86\%$, $R_1=2.03\%$, and $S=1.29$; they are much lower than those of the first analysis. Both of the split atoms O(31) and O(32) are located with equal occupancy on the b - c plane. The anisotropic thermal displacement parameters show that the O(1) atom has large U_{33} (c direction) and O(2) atom has large U_{22} (b direction) and U_{11} (a direction), which might reflect the thermal motion of ZnO₄ and PO₄ tetrahedra, which will be discussed later.

The results of the Rietveld analysis for phase II are tabulated in Tables III and IV, and shown in Fig. 1(b). In the analysis, the structure parameters with anisotropic atomic displacement reported by Blum *et al.*³ were used for the initial structure. In the case of phase II, the y coordinate of Zn

TABLE II. Anisotropic thermal displacement parameters (Å²) of phase I (disordered model).

Atoms	U_{11} (σ)	U_{22} (σ)	U_{33} (σ)	U_{12} (σ)	U_{13} (σ)	U_{23} (σ)
Cs	0.0364 (7)	0.0346 (6)	0.0396 (7)	0	-0.004 (11)	0
Zn	0.021 (1)	0.022 (1)	0.023 (1)	0	0.04 (1)	0
P	0.020 (3)	0.042 (3)	0.035 (3)	0	0.03 (3)	0
O(1)	0.035 (6)	0.041 (9)	0.139 (9)	0	-0.014 (8)	0
O(2)	0.16 (1)	0.18 (1)	0.04 (1)	0	0.029 (7)	0

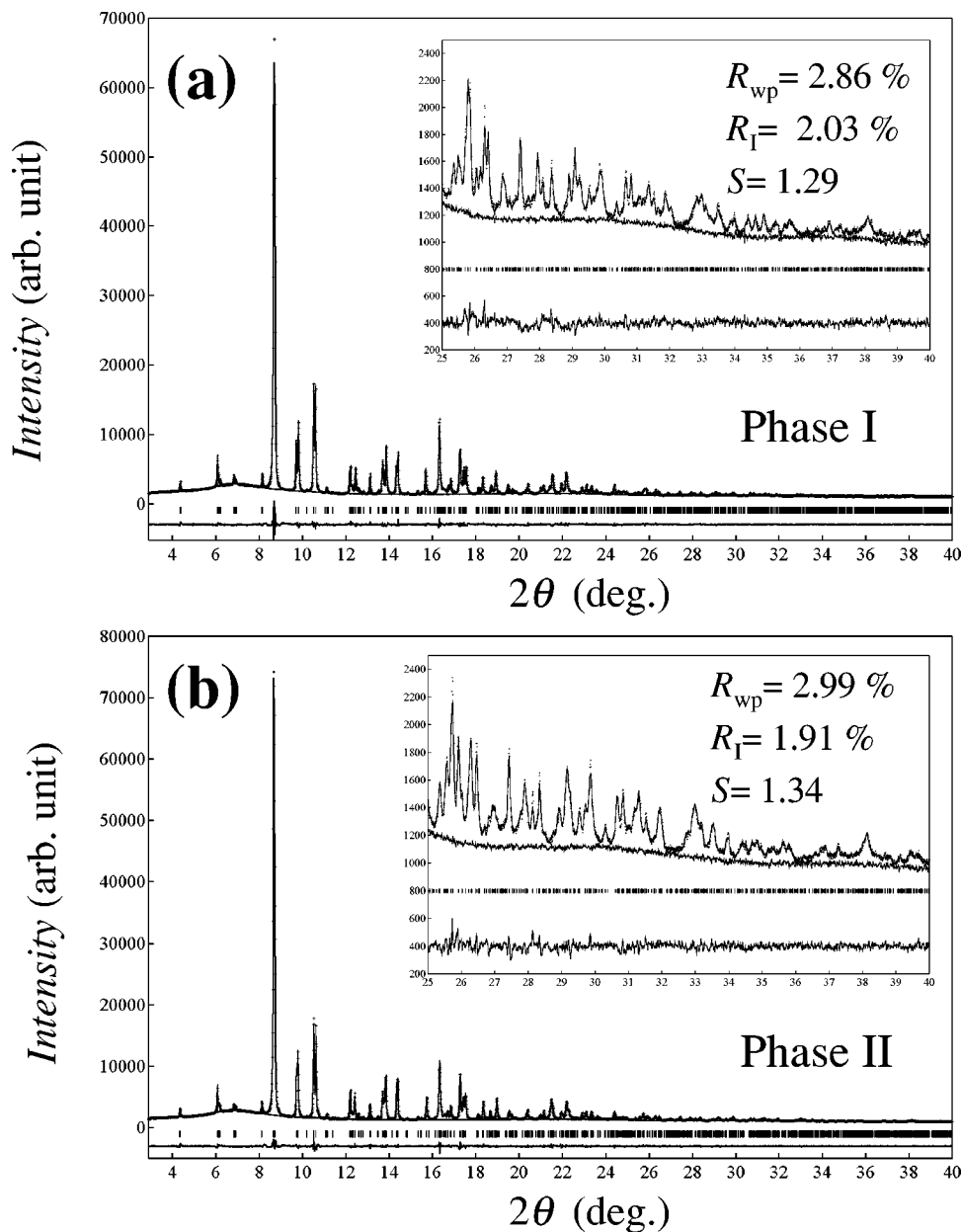


FIG. 1. Results of x-ray diffractometry and of Rietveld analysis of phase I at 613 K (a) and phase II at 553 K (b) of CZP. Dots: data. Solid lines: background. Bars: angular position of possible Bragg reflections. Plots at bottom: $(I_{\text{calc}} - I_{\text{obs}})$ difference. The data up to $2\theta = 40^\circ$ are corresponding to 0.73 \AA in d spacing.

has been fixed to 0.25 through the refinements.³ The reliability factors are $R_{\text{wp}} = 2.99\%$, $R_l = 1.91\%$, and $S = 1.34$ for phase II. The refined structure is in good agreement with that of Blum *et al.*,³ and no anomalous feature was observed in the difference Fourier synthesis map.²²

In order to study the structure concerning the I-II phase transition in detail, the maximum entropy method²³ was applied for phases I and II. So far, the MEM analysis has been successfully applied for structural studies of high-temperature superconductors,²⁴ fullerenes,²⁵ zeolites,²⁶ ferroelectrics,²⁷ etc., as the accurate electron density distribution could be obtained from a limited information of diffraction data.²⁸ In the present study, the observed structure factor F_{obs} and its standard deviation σ of the final results of the Rietveld analysis were used, and the MEM analysis was carried out with the unit cell divided into $90 \times 50 \times 90$ and $90 \times 50 \times 80$ pixels for phase I and phase II, respectively.

From the obtained electron density distribution, a three-dimensional equidensity surface ($0.6e \text{ \AA}^{-3}$) is drawn for phase I (Fig. 2). A relatively high electron density is seen on P-O and Zn-O bonds, which means that the PO_4 and ZnO_4 tetrahedra are formed with covalent bonds. On the other hand, a very low electron density is around the Cs cation, which means the ionic-bonding nature. It has been reported that the related compounds KZnPO_4 (Ref. 29) and TlZnPO_4 (Ref. 30) show relatively high ionic conduction. The alkali-metal ions in such a large cavity indicated by the present MEM analysis might be responsible for the high ionic conductivity.

Figure 3 shows the MEM electron density distribution in phase I at 613 K (a) and phase II at 553 K (b) on the plane of $x = 0.75$, which is indicated by the dotted line in Fig. 2. In Fig. 3, the contour lines are drawn from $0.1e \text{ \AA}^{-3}$ to $6.0e \text{ \AA}^{-3}$ with $0.3e \text{ \AA}^{-3}$ intervals. The split O(31) and O(32)

TABLE III. Results of the Rietveld analysis of phase II. $Pn2_1a$ $a=9.2500$ (4) Å, $b=5.4532$ (2) Å, $c=9.3176$ (4) Å, and $T=553$ K. The form of the anisotropic temperature factor is $\exp[-2\pi^2(h^2a^{*2}U_{11} + k^2b^{*2}U_{22} + l^2c^{*2}U_{33} + 2hka^*b^*U_{12} + 2hla^*c^*U_{13} + 2klb^*c^*U_{23})]$.

Site	g	Atoms	x (σ)	y (σ)	z (σ)	U_{eq} (10^{-2} Å ²)
4c	1.0	Cs	0.0028 (2)	0.250 (2)	0.1971 (1)	3.3
4c	1.0	Zn	0.1714 (2)	0.25	0.5842 (3)	1.9
4c	1.0	P	-0.1935 (5)	0.233 (3)	-0.4104 (8)	2.0
4c	1.0	O1	-0.030 (1)	0.26 (1)	-0.3957 (9)	7.3
4c	1.0	O2	-0.264 (1)	0.184 (4)	-0.278 (2)	6.9
4c	1.0	O3	0.250 (1)	0.007 (3)	0.457 (2)	2.7
4c	1.0	O4	-0.238 (1)	0.080 (3)	-0.528 (2)	4.0

atoms are clearly seen in Fig. 3(a), which are indicated by the arrows. The electron density maxima are observed at the positions of the split oxygen atoms, and the maximum values are $5.4e \text{ \AA}^{-3}$ for O(31) and $5.6e \text{ \AA}^{-3}$ for O(32). From the MEM electron density map, we conclude that the oxygen atoms are disordered with equal occupancy at O(31) and O(32) sites in phase I.

The mechanism of the I-II phase transition can be considered from Fig. 3. Assuming rigid tetrahedra of PO_4 and ZnO_4 , two disordered sites are possible with respect to the orientations of the tetrahedra in phase I. The PO_4 and ZnO_4 tetrahedra are ordered at one site in phase II, where the O(3) and O(4) atoms in phase II correspond to O(31) and O(32) atoms in phase I, respectively.

The relatively low electron density is observed for O(2) atoms: about $4.0e \text{ \AA}^{-3}$ at the maximum. This corresponds to the large thermal displacements indicated by the large U_{22} (b direction) and U_{11} (a direction) values, as given in Table II. The large U_{22} value of the O(2) atom is attributed to the reorientation motion of the tetrahedra between the O(31) and O(32) sites. The large U_{11} value of the O(2) atom in phase I also implies other thermal motions. Taking into account the large U_{33} (c direction) value of the O(1) atom, the librational motions of the PO_4 and ZnO_4 tetrahedra along with the O(31)-O(32) axis is a candidate for thermal motions. A similar librational thermal motion is observed also in phase II: the large U_{33} value of the O(1) atom and the U_{11} value of the O(2) atom, as given in Table IV. The slightly higher electron density distribution is observed along the P-O(2) bond compared with the other P-O bond in phases I and II. The bond length of P-O(2) is about 6% shorter than the others: 1.51 Å, 1.43 Å, 1.53 Å, and 1.54 Å for P-O(1), P-O(2), P-O(31), and

P-O(32), respectively. Such a covalent-bonding nature of P-O(2), including Zn-O(2), should be related to the large thermal displacement of the O(2) atom perpendicular to the covalent bond.

The thermal properties of CZP were studied by DSC between 300 K and 673 K with a scanning rate of $\pm 5 \text{ K min}^{-1}$. The DSC traces are shown in Fig. 4, where two anomalies are clearly seen due to the phase transitions of I-II and II-III. A substantial supercooling is seen for the II-III phase transition, which indicates that the II-III phase transition is of first order. The II-III phase transition is attributed to the so-called ferroelastic phase transition.² In the case of the I-II phase transition, no supercooling phenomenon was observed. The phase transition temperatures were determined from the heating run: 531 K for the II-III phase transition and 584 K for the I-II phase transition are in good agreement with a previous report.² The transition enthalpy and entropy are 105 J mol^{-1} and $0.2 \text{ J K}^{-1} \text{ mol}^{-1}$ for the II-III phase transition and 715 J mol^{-1} and $1.2 \text{ J K}^{-1} \text{ mol}^{-1}$ for the I-II phase transition, respectively.

The structure of the highest-temperature phase I is a prototype of phase II. A group theoretical analysis suggests that the averaged tilt angle of tetrahedra can be taken as the primary order parameter for the I-II phase transition, according to the irreducible representation Γ_4^- of $Pnma$.³¹ Since the irreducible representation Γ_4^- does not allow the construction of a Landau third-order invariant and a Lifshitz invariant, the order parameter should vary continuously at the transition temperature. In other words, a second-order phase transition is possible for the I-II phase transition. In the case of second-order phase transitions, the order parameter may vary

TABLE IV. Anisotropic thermal displacement parameters (Å²) of phase II.

Atoms	U_{11} (σ)	U_{22} (σ)	U_{33} (σ)	U_{12} (σ)	U_{13} (σ)	U_{23} (σ)
Cs	0.0316 (6)	0.0320 (6)	0.0371 (8)	-0.002 (6)	0.001 (1)	-0.0003 (30)
Zn	0.018 (1)	0.014 (1)	0.025 (1)	-0.012 (4)	-0.002 (1)	0.015 (4)
P	0.014 (3)	0.024 (3)	0.023 (3)	0.003 (6)	-0.0007 (27)	0.010 (6)
O(1)	0.022 (7)	0.06 (1)	0.12 (1)	-0.01 (2)	0.012 (9)	-0.09 (1)
O(2)	0.12 (2)	0.08 (2)	0.01 (1)	-0.03 (1)	-0.003 (7)	-0.02 (1)
O(3)	0.04 (2)	0.0003 (61)	0.04 (1)	-0.001 (8)	0.025 (7)	-0.009 (9)
O(4)	0.05 (2)	0.006 (8)	0.05 (1)	-0.008 (6)	0.009 (9)	-0.003 (9)

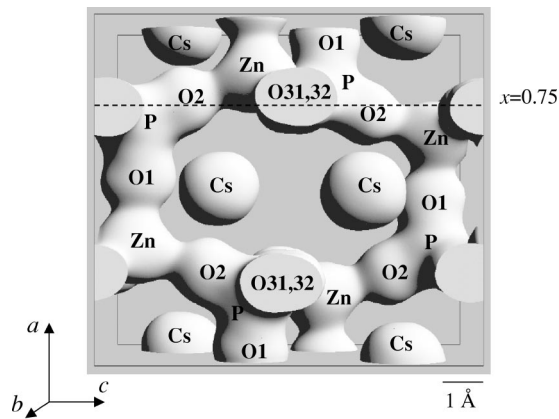


FIG. 2. Three-dimensional equidensity surface ($0.6e \text{ \AA}^{-3}$) of phase I at 613 K obtained by the MEM analysis.

smoothly without a discontinuous change. This might be the reason for the small entropy of the phase transition obtained by DSC, comparing with the value of $R \ln 2$ expected for the order-disorder type of phase transition.

From the viewpoint of the symmetry change at the I-II phase transition, phase II can be classified as a proper ferroelectric Aizu species $mmmFm2m$,³² and the spontaneous polarization parallel to the b axis is a candidate for the primary order parameter. However, the temperature dependence of the permittivity does not follow the Curie-Weiss law.² The similar compound ALS is so-called weak ferroelectrics and a pseudoproper ferroelectric transition is considered.¹⁰ In the case of CZP, phase II may be weak ferroelectrics and the I-II phase transition may be so-called weak ferroelectric transitions with the primary order parameter given by the orientation ordering of ZnO_4 and PO_4 tetrahedra and the spontaneous polarization may be result from the coupling with the primary order parameter.

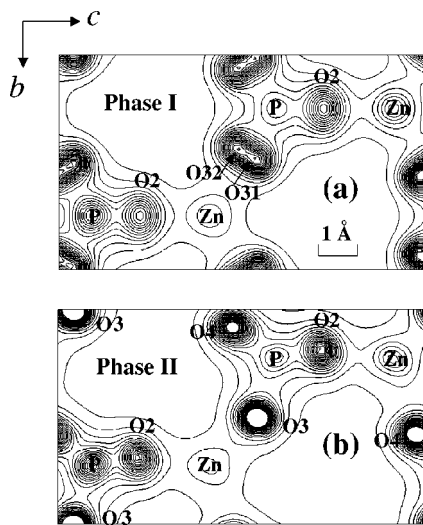


FIG. 3. The MEM electron density distribution in phase I at 613 K (a) and phase II at 553 K (b) on the plane of $x=0.75$. The contour lines are drawn from $0.1e \text{ \AA}^{-3}$ to $6.0e \text{ \AA}^{-3}$ with $0.3e \text{ \AA}^{-3}$ intervals. The split oxygen atoms O(31) and O(32) are indicated by arrows.

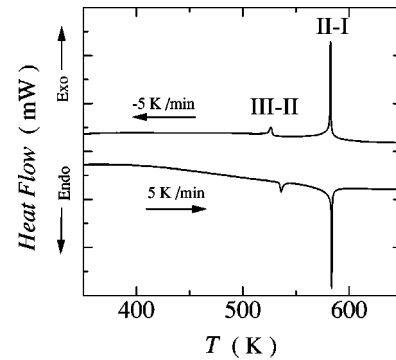


FIG. 4. DSC traces of CZP with scanning rate $\pm 5 \text{ K min}^{-1}$.

Although a clear disorder nature was observed in O(31) and O(32) atoms, large anisotropic thermal motion was found only in O(1) and O(2) atoms. If the mechanism is an order-disorder type of second-order phase transition, the heat capacity anomaly should be well explained by mean field theory (Bragg-Williams approximation).³³ However, the DSC trace showed a very sharp thermal anomaly at the I-II phase transition. Therefore a short-range interaction may be also responsible for the mechanism. Therefore, the I-II phase transition has the nature of not only order-disorder type, but also displacive type, and the intermediate nature between order-disorder type and displacive type should be considered. According to the rigid ZnO_4 , PO_4 model, disordering of O(2) atoms should be observed. However, no disorder site was observed in the O(2) atom and a short bond length and high electron density distribution are observed in the P-O(2) bond. Such an anomalous nature in the P-O(2) bond may be responsible for the order nature in O(2) atoms of phase I in CZP. Such an intermediate nature between order-disorder type and displacive may be an intrinsic feature of I-II phase transitions.

IV. CONCLUSION

The I-II phase transition in CsZnPO_4 was studied by x-ray powder diffractometry with high-energy synchrotron radiation and by DSC. The Rietveld analysis of the diffraction data and the electron density studies by the MEM showed substantial disorder at oxygen sites in the highest-temperature phase I. From the DSC, the transition enthalpy and entropy were estimated as 715 J mol^{-1} and $1.2 \text{ J mol}^{-1} \text{ K}^{-1}$, respectively. The transition entropy is comparable with $R \ln 2$ expected for the order-disorder mechanism. It is concluded that phase I is in a disordered state with respect to the orientation ordering of PO_4 and ZnO_4 tetrahedra. Phase II might be a weak ferroelectrics and the I-II phase transition is so-called weak ferroelectric transitions with the primary order parameter of orientation ordering of ZnO_4 and PO_4 tetrahedra and the mechanism should be of an intermediate nature between order-disorder type and displacive type.

ACKNOWLEDGMENTS

The authors thank S. Aoyagi for his help in the experiments at SPring-8 and in the MEM analysis. The experi-

ments at SPring-8 were performed with the approval of the Japan Synchrotron Radiation Research Institute (JASRI) (Proposal No. 2001B0389-ND-np).

-
- ¹B. Elouadi and L. Elammari, *Ferroelectrics* **107**, 253 (1990).
²D. Blum, J. C. Peuzin, and J. Y. Henry, *Ferroelectrics* **61**, 265 (1984).
³D. Blum, A. Durif, and M. T. Averbuch-Pouchot, *Ferroelectrics* **69**, 283 (1986).
⁴A. Sawada, T. Azumi, and Y. Kuroiwa, *Ferroelectrics* **237**, 245 (2000).
⁵I. Yamashita, T. Tojo, H. Kawaji, and T. Atake, *Phys. Rev. B* **65**, 212 104 (2002).
⁶W. A. Dollase, *Acta Crystallogr., Sect. B: Struct. Crystallogr. Cryst. Chem.* **25**, 2298 (1969).
⁷H. Mashiyama and H. Kasano, *J. Phys. Soc. Jpn.* **62**, 155 (1993).
⁸K. Itoh, H. Ishikura, and E. Nakamura, *Acta Crystallogr., Sect. B: Struct. Crystallogr. Cryst. Chem.* **37**, 664 (1981).
⁹K. Hasebe and T. Asahi, *Phys. Rev. B* **41**, 6794 (1990).
¹⁰M. Polomska, *Phase Transitions* **74**, 409 (2001).
¹¹M. Horioka, A. Sawada, and M. Wada, *J. Phys. Soc. Jpn.* **58**, 3793 (1989).
¹²H. Yanagihara, M. Horioka, S. Furuta, and T. Yamaguchi, *J. Phys. Soc. Jpn.* **65**, 1099 (1996).
¹³M. Wada, A. Sawada, and Y. Ishibashi, *J. Phys. Soc. Jpn.* **50**, 1981 (1981).
¹⁴M. Wada, K. Fujita, A. Sawada, and Y. Ishibashi, *Jpn. J. Appl. Phys., Part 1* **24**, S488 (1985).
¹⁵K. Deguchi, N. Aramaki, E. Nakamura, and K. Tanaka, *J. Phys. Soc. Jpn.* **52**, 1897 (1983).
¹⁶J. F. Scott and G. E. Feldkamp, *Ferroelectrics* **52**, 211 (1983).
¹⁷M. Sugo, M. Kasahara, M. Tokunaga, and I. Tatsuzaki, *J. Phys. Soc. Jpn.* **53**, 3234 (1984).
¹⁸E. Nishibori, M. Takata, K. Kato, M. Sataka, Y. Kubota, S. Aoyagi, Y. Kuroiwa, M. Yamakata, and N. Ikeda, *Nucl. Instrum. Methods Phys. Res. A* **467-468**, 1045 (2001).
¹⁹H. M. Rietveld, *J. Appl. Crystallogr.* **2**, 65 (1969).
²⁰F. Izumi and T. Ikeda, *Mater. Sci. Forum* **321-324**, 198 (2000).
²¹S. Kumazawa, Y. Kubota, M. Takata, and M. Sakata, *J. Appl. Crystallogr.* **26**, 453 (1993).
²²R. A. Young, *The Rietveld Method* (Oxford University Press, Oxford, 1993).
²³M. Sakata and M. Sato, *Acta Crystallogr., Sect. A: Found. Crystallogr.* **46**, 263 (1990).
²⁴M. Takata, E. Nishibori, T. Takayama, M. Sakata, K. Komada, M. Sato, and C. J. Howard, *Physica C* **262**, 176 (1996).
²⁵M. Takata, B. Umeda, E. Nishibori, M. Sakata, Y. Saito, M. Ohno, and H. Shinohara, *Nature (London)* **377**, 46 (1995).
²⁶R. J. Papoular and D. E. Cox, *Europhys. Lett.* **32**, 337 (1995).
²⁷Y. Kuroiwa, S. Aoyagi, A. Sawada, J. Harada, E. Nishibori, M. Takata, and M. Sakata, *Phys. Rev. Lett.* **87**, 217601 (2001).
²⁸M. Takata, E. Nishibori, and M. Sakata, *Z. Kristallogr.* **216**, 71 (2001).
²⁹G. Wallez, F. Lucas, J.-P. Sournon, and M. Quarton, *Mater. Res. Bull.* **34**, 1251 (1999).
³⁰M. Andratschke, *Z. Anorg. Allg. Chem.* **620**, 361 (1994).
³¹V. Kahlenberg, *Z. Kristallogr.* **213**, 13 (1998).
³²K. Aizu, *J. Phys. Soc. Jpn.* **27**, 387 (1969).
³³K. Morikawa, T. Atake, M. Wadaa, and T. Yamaguchi, *J. Phys. Soc. Jpn.* **67**, 1994 (1998).